

# MATHEMATICAL MODELLING OF AN AUTONOMOUS VEHICLE FOR NAVIGATION CONTROL

Katsumi Moriwaki<sup>1</sup> and Katsuyuki Tanaka<sup>1</sup>

<sup>1</sup>The University of Shiga Prefecture, School of Mechanical Systems Engineering  
2500 Hasaka-cho, Hikone, Shiga, Japan  
*moriwaki@mech.usp.ac.jp* (Katsumi Moriwaki)

## Abstract

The problem of modelling and control for autonomous vehicles is considered. Mutual interactions among vehicle motion dynamics are evaluated. It is proposed the mathematical model suitable for describing and simulating the whole motion of autonomous passenger vehicles. The passenger vehicles are evaluated from many points of views, such as riding comfort, vehicle position, stability, manipulability and so on. The performance of vehicle control in technically is separated into several control items and considered to each item independently. The mathematical model for steering control of an autonomous vehicle has usually two degrees of freedom, which consider the lateral motion and the yawing motion. The model for suspension dynamics, which is deeply related to riding comfort, has also two degrees of freedom, which consider the bouncing motion and the pitching motion. The above mentioned models are not enough to treat the problem of total motion control of autonomous vehicles. The specifications of tires must also be considered in the whole motion control of vehicles and they have strong nonlinearity. There are, furthermore, mutual interactions among them, which are inevitably considered when the problem of the whole motion control of autonomous passenger vehicles.

**Keywords:** Autonomous vehicle, Motion dynamics, Navigation, Guidance control, Robust control.

## Presenting Author's Biography

Katsumi Moriwaki. He received the B.E. degree in Mechanical Engineering from Kyoto Institute of Technology in 1975, both of the M.E. degree in Precision Mechanics and the Ph.D. degrees in Applied Mathematics from Kyoto University in 1977 and 1996. He was with the Department of Mechanics, Osaka Municipal Technical Research Institute from 1980 to 1989. From 1989 to 1995, he was with the Department of Mechanical Engineering, Shiga Prefectural Junior College. In 1995, he joined the Department of Mechanical Systems Engineering, School of Engineering, The University of Shiga Prefecture, where he is currently working in the areas of automatic control and robotics.



## 1 Introduction

The passenger vehicles are evaluated from many points of views, such as riding comfort, vehicle position, stability, manipulability and so on (Fig. 1). In the recent year, the electric control systems of chassis functions – suspension, steering, drivetrain and brake – have been developed rapidly. These systems have been developed for the purpose of obtaining the maximum performance independently [1].

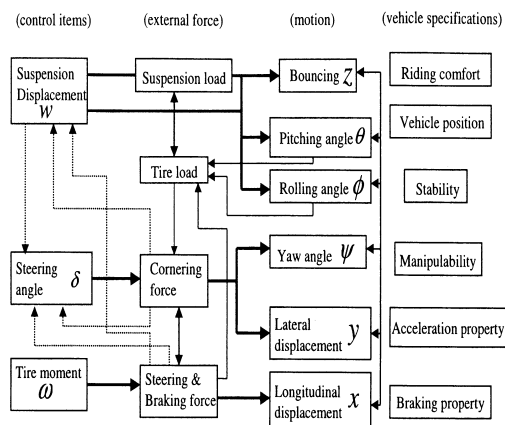


Fig. 1 Integrated vehicle control [1]

The performance of vehicle control is technically separated into several control items and considered to each item independently, too. The mathematical model for steering control of an autonomous vehicle has usually two degrees of freedom, which consider the lateral motion and the yawing motion [2, 3]. The model for suspension dynamics, which is deeply related to riding comfort, has also two degrees of freedom, which consider the bouncing motion and the pitching motion [4, 5]. The above mentioned models are not enough to treat the problem of total motion control for autonomous vehicles. The specifications of tires must also be considered in the whole motion control of vehicles and they have strong nonlinearity [6]. There are, furthermore, mutual interactions among them, which are inevitably to be taken into account in the problem of the whole motion control for autonomous passenger vehicles (Fig. 2).

## 2 Modelling of an autonomous vehicles

### 2.1 Steering model of an autonomous vehicle

The features of car steering dynamics in a horizontal plane are described by Fig. 3 [3, 4, 5, 6, 7]. In Fig. 3, the angle  $\delta$  is the front steering angle and the angles  $\beta_{f1}, \beta_{f2}, \beta_{r1}, \beta_{r2}$  are the sideslip angles of front tires and rear tires, respectively.

The angle  $\beta$  between the vehicle center line and the velocity vector  $V$  is called “vehicle sideslip angle”. The

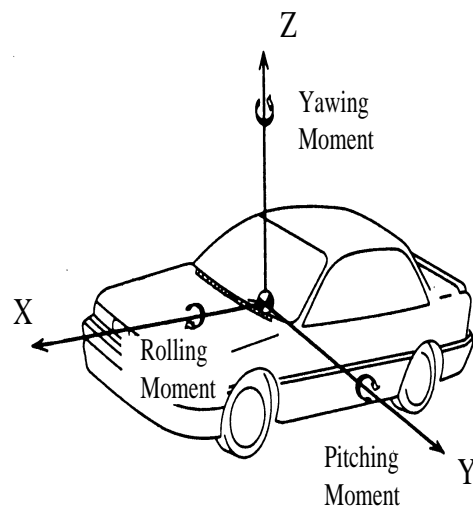


Fig. 2 Rigid-body model of four wheel vehicles

cornering forces  $Y_{f1}, Y_{f2}, Y_{r1}, Y_{r2}$  are the forces transmitted from the road surface via the wheels to the car chassis. The distance between the center of gravity (P) and the front axle (resp. rear axle) is  $l_f$  (resp.  $l_r$ ) and together  $l = l_f + l_r$  is the wheel base. In the horizontal plane of Fig. 3 an inertially fixed coordinate system  $(X, Y)$  is shown together with a vehicle fixed coordinate system  $(x, y)$  that is rotated by a “yaw angle”  $\psi$ . In the dynamic equations the yaw rate  $r := \dot{\psi}$  will appear as a state variable.

Assuming that  $\beta_f = \beta_{f1} = \beta_{f2} = \delta - \beta - l_f r / V$ ,  $\beta_r = \beta_{r1} = \beta_{r2} = -\beta + l_r r / V$ , and  $|\beta_f| \ll 1$ ,  $|\beta_r| \ll 1$ ,  $|\delta| \ll 1$ , then the “two wheel model” [8] (Fig. 4) can be regarded as the equivalent model to the four wheel model (Fig. 3).

The side forces  $f_f := 2Y_f$ ,  $f_r := 2Y_r$  are projected through the steering angle into chassis coordinate  $(x, y)$ , where they appear as forces  $f_x, f_y$  and the torque  $m_z$  around a  $z$ -axis which is pointing upward from the center of gravity (P).

$$\begin{bmatrix} f_x \\ f_y \\ m_z \end{bmatrix} = \begin{bmatrix} -\sin \delta & 0 \\ \cos \delta & 1 \\ l_f \cos \delta & -l_r \end{bmatrix} \begin{bmatrix} f_f \\ f_r \end{bmatrix} \quad (1)$$

Via the dynamics model the forces cause state variables  $\beta, V, r$ . The equations of motions for three degrees of freedom in the horizontal plane are

#### 1. longitudinal motion

$$-mV(\dot{\beta} + r) \sin \beta + m\dot{V} \cos \beta = f_x \quad (2)$$

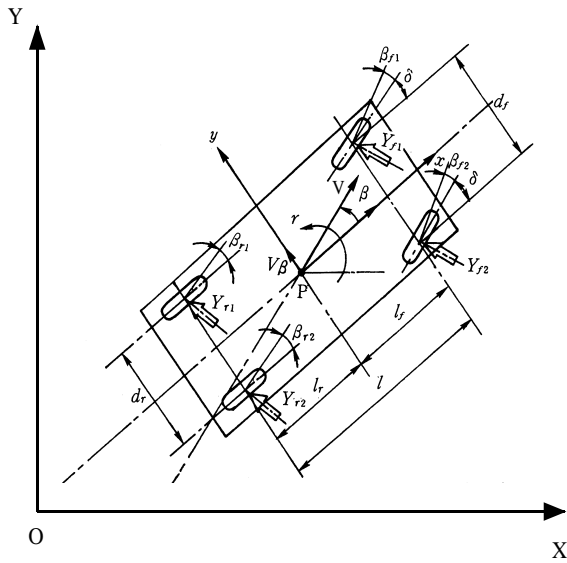


Fig. 3 Four wheel model for car steering

2. lateral motion

$$mV(\dot{\beta} + r) \cos \beta + m\dot{V} \sin \beta = f_y \quad (3)$$

3. yaw motion

$$I\dot{r} = m_z \quad (4)$$

It is obtained that from Eq.(2) to Eq.(4)

$$\begin{bmatrix} mV(\dot{\beta} + r) \\ m\dot{V} \\ I\dot{r} \end{bmatrix} = \begin{bmatrix} -\sin \beta & \cos \beta & 0 \\ \cos \beta & \sin \beta & 0 \\ 0 & 0 & 1 \end{bmatrix} \times \begin{bmatrix} f_x \\ f_y \\ m_z \end{bmatrix} \quad (5)$$

The side force  $f_y$  is known to be the nonlinear function of the tire sideslip angles  $\beta_f, \beta_r$ , i.e.,

$$f_y = f_f(\beta_f) + f_r(\beta_r) \quad (6)$$

Two wheel model (5) and (6) is nonlinear and we will introduce the additional assumptions[3] as follows.

(A1) The sideslip angle  $\beta$  is assumed to be small. Then, Eq.(5) becomes

$$\begin{bmatrix} mV(\dot{\beta} + r) \\ m\dot{V} \\ I\dot{r} \end{bmatrix} = \begin{bmatrix} -\beta & 1 & 0 \\ 1 & \beta & 0 \\ 0 & 0 & 1 \end{bmatrix} \begin{bmatrix} f_x \\ f_y \\ m_z \end{bmatrix} \quad (7)$$

(A2) The velocity is constant,  $\dot{V} = 0$ . Then, the second row of Eq.(7) yields  $f_x = -\beta f_y$  and with  $\beta^2 \ll 1$ , then we have

$$\begin{bmatrix} mV(\dot{\beta} + r) \\ I\dot{r} \end{bmatrix} = \begin{bmatrix} 1 & 0 \\ 0 & 1 \end{bmatrix} \begin{bmatrix} f_y \\ m_z \end{bmatrix} \quad (8)$$

The velocity  $V$  is treated as an uncertain constant parameter.

(A3) The nonlinear characteristic of Eq.(6) is approximated by the nominal value of the tangent at  $\beta_f = \beta_r = 0$  and small nonlinear functions, i.e.,

$$\begin{aligned} f_f(\beta_f) &= c_f \mu(\beta_f + \Delta_1(\beta, r)) \\ f_r(\beta_r) &= c_r \mu(\beta_r + \Delta_2(\beta, r)) \end{aligned} \quad (9)$$

where  $\Delta_i(\beta, r)$ , ( $i = 1, 2$ ) is  $C^\infty$  nonlinear function and  $|\Delta_i(\beta, r)| \ll 1$  [8, 9]. The constant coefficients

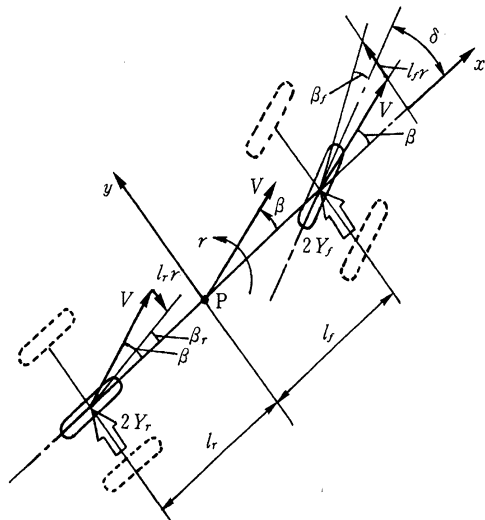


Fig. 4 Two wheel model for car steering

$c_f, c_r$  are called “cornering stiffness”, and  $\mu$  is the adhesion factor (treated here as a disturbance) between road surface and tire. Typical experimental values of  $\mu$  [3] are

$$\begin{aligned} \mu &= 1 && \text{dry road} \\ \mu &= 0.5 && \text{wet road} \\ \mu &= 0.15 && \text{ice.} \end{aligned}$$

The steering model follows from Eq.(7) to Eq.(9) and using Eq.(1) as

$$\begin{bmatrix} mV(\dot{\beta} + r) \\ I\dot{r} \end{bmatrix} = \begin{bmatrix} 1 & 1 \\ l_f & -l_r \end{bmatrix} \times \begin{bmatrix} c_f\mu(\delta - \beta - l_f r/V + \Delta_1(\beta, r)) \\ c_r\mu(-\beta + l_r r/V + \Delta_2(\beta, r)) \end{bmatrix} \quad (10)$$

The uncertain parameters in this model are mass  $m$ , moment of inertia  $I$ , velocity  $V$  and road friction factor  $\mu$ . Solving Eq.(10) for  $\dot{\beta}$  and  $\dot{r}$  and rearranging terms yields the nonlinear state space model

$$\begin{bmatrix} \dot{\beta} \\ \dot{r} \end{bmatrix} = \begin{bmatrix} a_{11} & a_{12} \\ a_{21} & a_{22} \end{bmatrix} \begin{bmatrix} \beta \\ r \end{bmatrix} + \begin{bmatrix} b_1 \\ b_2 \end{bmatrix} \delta + \begin{bmatrix} g_1(\beta, r) \\ g_2(\beta, r) \end{bmatrix} \mu \quad (11)$$

where

$$\begin{aligned} a_{11} &= -\frac{c_f + c_r}{mV}, & a_{12} &= -1 + \frac{c_r l_r - c_f l_f}{mV^2} \\ a_{21} &= \frac{c_r l_r - c_f l_f}{I}, & a_{22} &= -\frac{c_f l_f^2 + c_r l_r^2}{IV} \\ b_1 &= \frac{c_f}{mV}, & b_2 &= \frac{c_f l_f}{I} \\ \tilde{m} &:= \frac{m}{\mu}, & \tilde{I} &:= \frac{I}{\mu} \end{aligned}$$

and

$$\begin{aligned} g_1(\beta, r) &= c_f \Delta_1(\beta, r) + c_r \Delta_2(\beta, r), \\ g_2(\beta, r) &= l_f c_f \Delta_1(\beta, r) - l_r c_r \Delta_2(\beta, r) \end{aligned}$$

## 2.2 Geometric model of steering motion for $|V| < 1$ .

The steering motion of autonomous vehicles with low velocity ( $|V| \approx 0$ ) can not be described by Eq.(11), because some coefficients of Eq.(11) include  $V$  in their denominators. In this case there can be assumed to be no sideslip angle ( $\beta \equiv 0$ ) and the velocity vector of P is given by  $(V, 0)$  in a vehicle fixed coordinate system  $(x, y)$  with the yaw rate :

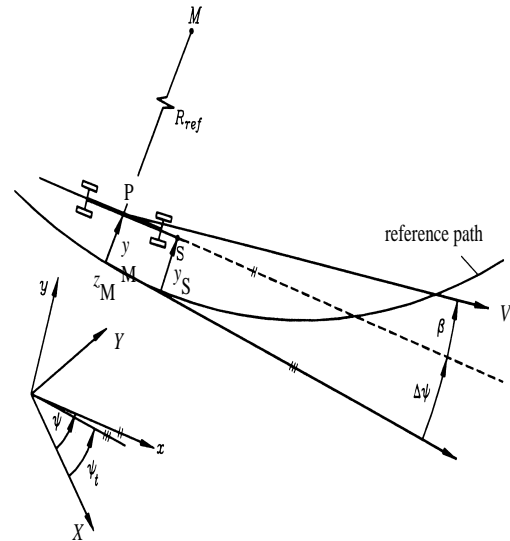


Fig. 5 Scheme of automatic vehicle steering

$$r = \frac{V}{l} \tan \delta \quad (12)$$

## 2.3 Suspension model of an autonomous vehicle

The features of car vertical dynamics in  $(X-Z)$ -plane are described by Fig. 6[4, 5, 6] with active suspension system in which the external control forces is used to suppress the uncomfortable bouncing motion and pitching motion.

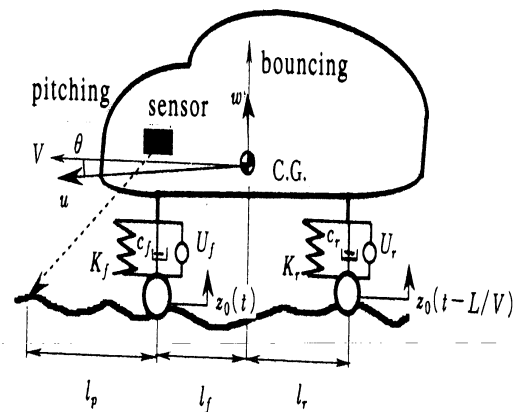


Fig. 6 Active suspension control[5]

The equations of motions for two degrees of freedom in  $(X-Z)$ -plane with the constant velocity  $V$  are

## i. bouncing motion

$$m\ddot{z} = F_f + F_r \quad (13)$$

## ii. pitching motion

$$I_y \ddot{\theta} = -l_f F_f + l_r F_r \quad (14)$$

where  $z$  is the vertical displacement of the center of gravity (CG) of a car (Fig. 6),  $\theta$  is the pitching angle of the center of gravity (CG) of a car and the external forces acting on a front wheel and the rear wheel from the road surface are written by  $F_f$  and  $F_r$ , respectively. The state space model of the vertical dynamics is derived from Eqs.(13), (14) as follows[5].

$$\begin{aligned} \begin{bmatrix} \dot{z} \\ \dot{\theta} \\ \dot{w} \\ \dot{q} \end{bmatrix} &= \begin{bmatrix} 0 & 0 & 1 & 0 \\ 0 & 0 & 0 & 1 \\ \tilde{a}_{31} & \tilde{a}_{32} & \tilde{a}_{33} & \tilde{a}_{34} \\ \tilde{a}_{41} & \tilde{a}_{42} & \tilde{a}_{43} & \tilde{a}_{44} \end{bmatrix} \begin{bmatrix} z \\ \theta \\ w \\ q \end{bmatrix} \\ &+ \begin{bmatrix} 0 & 0 \\ 0 & 0 \\ \tilde{b}_{31} & \tilde{b}_{32} \\ \tilde{b}_{41} & \tilde{b}_{42} \end{bmatrix} \begin{bmatrix} U_f \\ U_r \end{bmatrix} \\ &+ \begin{bmatrix} 0 & 0 \\ 0 & 0 \\ \tilde{h}_{31} & \tilde{h}_{32} \\ \tilde{h}_{41} & \tilde{h}_{42} \end{bmatrix} \begin{bmatrix} z_{of} \\ z_{or} \end{bmatrix} \end{aligned} \quad (15)$$

where  $w := \dot{z}$ ,  $q := \dot{\theta}$  and

$$\begin{aligned} \tilde{a}_{31} &= -\frac{K_f + K_r}{m}, & \tilde{a}_{32} &= \frac{K_f l_f - K_r l_r}{m} \\ \tilde{a}_{33} &= -\frac{C_f + C_r}{m}, & \tilde{a}_{34} &= \frac{C_f l_f - C_r l_r}{m} \\ \tilde{a}_{41} &= \frac{K_f l_f - K_r l_r}{I_y}, & \tilde{a}_{42} &= -\frac{K_f l_f^2 + K_r l_r^2}{I_y} \\ \tilde{a}_{43} &= \frac{C_f l_f - C_r l_r}{I_y}, & \tilde{a}_{44} &= -\frac{C_f l_f^2 + C_r l_r^2}{I_y} \\ \tilde{b}_{31} &= \frac{1}{m}, & \tilde{b}_{32} &= \frac{1}{m} \\ \tilde{b}_{41} &= -\frac{l_f}{I_y}, & \tilde{b}_{42} &= \frac{l_r}{I_y} \\ \tilde{h}_{31} &= \frac{K_f}{m}, & \tilde{h}_{32} &= \frac{K_r}{m} \\ \tilde{h}_{41} &= -\frac{K_f l_f}{I_y}, & \tilde{h}_{42} &= \frac{K_r l_r}{I_y} \end{aligned}$$

$K_f$  : stiffness coefficient for front suspension  
 $K_r$  : stiffness coefficient for rear suspension  
 $C_f$  : damping coefficient for front suspension  
 $C_r$  : damping coefficient for rear suspension

In Equation (15), the external input  $z_{of}$ ,  $z_{or}$  are assumed to be the random variations at the front tire and the rear tire, respectively, which are induced by the steering motion. According to Eqs. (9) and (11),  $z_{of}$ ,  $z_{or}$  are assumed to be induced as the form

$$\begin{aligned} z_{of} &= \sigma_f f_f(\beta_f) \\ z_{or} &= \sigma_r f_r(\beta_r) \end{aligned} \quad (16)$$

where  $\sigma_f$ ,  $\sigma_r$  are unknown coefficients. Using sensors for the height of CG of the car and the pitching angle of CG of the car, it can be assumed that the output equation for Eq. (15) is given by

$$\begin{bmatrix} w \\ q \end{bmatrix} = \begin{bmatrix} 0 & 0 & 1 & 0 \\ 0 & 0 & 0 & 1 \end{bmatrix} \begin{bmatrix} z \\ \theta \\ w \\ q \end{bmatrix} \quad (17)$$

### 3 Extended Model for Automatic Vehicle Control

#### 3.1 Extended state space model for vehicle steering

In order to consider the problem of automatic car steering, the extended model of vehicle is introduced. The extended model must include not only velocities, but also the vehicle heading and the lateral position of the sensor with respect to the reference path. This extended model is derived using a nonlinear model that is valid for deviations from a stationary path. It is assumed that the reference path is given as an arc with radius  $R_{\text{ref}}$  and center  $M$  (See Fig. 5)[3]. For a straight path segment the radius is  $R_{\text{ref}} = \infty$ . It is more convenient to introduce the curvature  $\rho_{\text{ref}} := 1/R_{\text{ref}}$  as input that generates the reference path. The curvature is defined positive for left cornering and negative for right cornering. The radial line from the center  $M$  passing through the center of gravity (P) of the vehicle intersects a unique point  $z_M$  on the desired path. It is assumed that there is a small deviation from the reference point  $z_M$  to the center of gravity which is the deviation  $y_p$  and that a vehicle fixed coordinate system  $(x, y)$  is rotated from the inertially fixed coordinate system  $(X, Y)$  by the yaw angle  $\psi$ . The tangent to the reference path at  $z_M$  is rotated by a reference yaw angle  $\psi_t$  with respect to  $X$ . Thus, the rate of change of  $y_p$  is given by  $V \sin(\beta + \Delta\psi)$  where  $\beta$  is the vehicle sideslip angle and  $\Delta\psi := \psi - \psi_t$  is the angle between the tangent to the reference path at  $z_M$  and the center line of the vehicle. With the linearization  $\sin(\beta + \Delta\psi) \approx \beta + \Delta\psi$  the deviation  $y_p$  changes according to

$$\dot{y}_p = V(\beta + \Delta\psi) \quad (18)$$

If the sensor S is mounted in a distance  $l_s$  in front of the center of gravity with  $l_s \ll R_{\text{ref}}$ , the measured deviation  $y_s$  from the reference path changes both with  $\dot{y}_p$  and under the influence of the yaw rate  $r = \dot{\psi}$ . Taking

this into account, the rate of change of the measured deviation is

$$\dot{y}_s = V(\beta + \Delta\psi) + l_s r \quad (19)$$

Determination of  $\dot{y}_s$  requires knowledge of three variables  $\beta$ ,  $r$  and  $\Delta\psi$ . The variables  $\beta$  and  $r$  are given by Eq.(11). The angle  $\Delta\psi$  will be obtained by

$$\Delta\dot{\psi} = r - V\rho_{\text{ref}} \quad (20)$$

Combining Eqs.(11), (19) and (20), the extended state space model is obtained as [2, 3, 9, 10].

$$\begin{aligned} \begin{bmatrix} \dot{\beta} \\ \dot{r} \\ \Delta\dot{\psi} \\ \dot{y}_s \end{bmatrix} &= \begin{bmatrix} a_{11} & a_{12} & 0 & 0 \\ a_{21} & a_{22} & 0 & 0 \\ 0 & 1 & 0 & 0 \\ V & l_s & V & 0 \end{bmatrix} \begin{bmatrix} \beta \\ r \\ \Delta\psi \\ y_s \end{bmatrix} \\ &+ \begin{bmatrix} b_1 \\ b_2 \\ 0 \\ 0 \end{bmatrix} \delta + \begin{bmatrix} 0 \\ 0 \\ -V \\ 0 \end{bmatrix} \rho_{\text{ref}} \\ &+ \begin{bmatrix} g_1(\beta, r) \\ g_2(\beta, r) \\ 0 \\ 0 \end{bmatrix} \mu \end{aligned} \quad (21)$$

Using sensors for the yaw rate  $r$  (ex. a gyro) and the deviation  $y_s$  (ex. a GPS), it can be assumed that the output equation for Eq.(21) is given by

$$\begin{bmatrix} \Delta\psi \\ y_s \end{bmatrix} = \begin{bmatrix} 0 & 0 & 1 & 0 \\ 0 & 0 & 0 & 1 \end{bmatrix} \begin{bmatrix} \beta \\ r \\ \Delta\psi \\ y_s \end{bmatrix} \quad (22)$$

The system (21), (22) with the control input  $\delta$ , the reference input  $\rho_{\text{ref}}$ , the disturbance input  $\mu$  and the output  $\Delta\psi, y_s$  is shown to be controllable and observable w.r.t.  $\delta$ .

### 3.2 State space model for the case : $|V| < 1$ , $|\dot{V}| < 1$

In this case, the automatic vehicle steering can be described by Eqs.(19) and (20)

$$\begin{aligned} \begin{bmatrix} \Delta\dot{\psi} \\ \dot{y}_s \end{bmatrix} &= \begin{bmatrix} 0 & 0 \\ V & 0 \end{bmatrix} \begin{bmatrix} \Delta\psi \\ y_s \end{bmatrix} + \begin{bmatrix} 1 \\ l_s \end{bmatrix} r \\ &+ \begin{bmatrix} -V \\ 0 \end{bmatrix} \rho_{\text{ref}} \end{aligned} \quad (23)$$

Substituting Eq.(12) into Eq.(23) with the approximation  $\tan \delta \approx \delta + w(\delta)$ , in which  $w(\delta)$  is small nonlinear function ( $\in C^\infty$ ), we have

$$\begin{aligned} \begin{bmatrix} \Delta\dot{\psi} \\ \dot{y}_s \end{bmatrix} &= \begin{bmatrix} 0 & 0 \\ V & 0 \end{bmatrix} \begin{bmatrix} \Delta\psi \\ y_s \end{bmatrix} + \frac{V}{l} \begin{bmatrix} 1 \\ l_s \end{bmatrix} \delta \\ &+ \begin{bmatrix} -V \\ 0 \end{bmatrix} \rho_{\text{ref}} + \frac{V}{l} \begin{bmatrix} 1 \\ l_s \end{bmatrix} w(\delta) \end{aligned} \quad (24)$$

Using sensors for the yaw rate  $r$  (ex. a gyro) and the deviation  $y_s$  (ex. a GPS), it can be assumed that the state variables of Eq.(24) is directly obtained. The system (24) with the control input  $\delta$  and the reference input  $\rho_{\text{ref}}$  is shown to be controllable.

## 4 Optimized Servo-Controllers for Automatic Vehicle Traveling

### 4.1 Nonlinear state feedback $H_\infty$ optimal controller

It is considered to design the  $H_\infty$  optimal controller so that the output  $[\Delta\psi^T, y_s^T]^T$  can be driven to zero as  $t \rightarrow \infty$  [2]. In this paper, the problem of  $H_\infty$  optimal control is considered so that the output  $[\Delta\psi^T, y_s^T]^T$  can be driven to zero as  $t \rightarrow \infty$  with the output  $[w^T, q^T]^T$  can be driven to zero as  $t \rightarrow \infty$ , which are related with the riding comfort. From the steering system (21), (22) with the suspension system (15), (17) and the steering system (23), (24) with the suspension system(15), (17), the vehicle system is able to be rewritten as the same form

$$\begin{aligned} \dot{x}_i(t) &= A_i x_i(t) + B_i u_i(t) + D_i \rho_{\text{ref}}(t) \\ &\quad + G_i(\Delta) d_i(t) \quad (25) \\ y(t) &= C_i x_i(t), \quad (i = 1, 2) \end{aligned}$$

where

$$\begin{aligned} x_1 &:= [\beta^T \ r^T \ \Delta\psi^T \ y_s^T \ | \ z^T \ \theta^T \ w^T \ q^T]^T, \\ &\quad \text{(for the case : } |V| > 1, |\dot{V}| < 1) \end{aligned}$$

$$\begin{aligned} x_2 &:= [\Delta\psi^T \ y_s^T \ | \ z^T \ \theta^T \ w^T \ q^T]^T, \\ &\quad \text{(for the case : } |V| < 1, |\dot{V}| < 1) \end{aligned}$$

$$u_i := [\delta^T \ | \ U_f^T \ U_r^T]^T, \quad (i = 1, 2)$$

and

$$d_1 := \mu \text{ (for the case : } |V| > 1, |\dot{V}| < 1)$$

$d_2 := w(\delta)$  (for the case  $\cdot$ ,  $|V| < 1$ ,  $|\dot{V}| < 1$ )

Each coefficient matrix is as follows.

$$A_1 = \text{diag}\left\{ \begin{bmatrix} a_{11} & a_{12} & 0 & 0 \\ a_{21} & a_{22} & 0 & 0 \\ 0 & 1 & 0 & 0 \\ V & l_s & V & 0 \end{bmatrix}, \begin{bmatrix} 0 & 0 & 1 & 0 \\ 0 & 0 & 0 & 1 \\ \tilde{a}_{31} & \tilde{a}_{32} & \tilde{a}_{33} & \tilde{a}_{34} \\ \tilde{a}_{41} & \tilde{a}_{42} & \tilde{a}_{43} & \tilde{a}_{44} \end{bmatrix} \right\}$$

$$A_2 = \text{diag}\left\{ \begin{bmatrix} 0 & 0 \\ V & 0 \end{bmatrix}, \begin{bmatrix} 0 & 0 & 1 & 0 \\ 0 & 0 & 0 & 1 \\ \tilde{a}_{31} & \tilde{a}_{32} & \tilde{a}_{33} & \tilde{a}_{34} \\ \tilde{a}_{41} & \tilde{a}_{42} & \tilde{a}_{43} & \tilde{a}_{44} \end{bmatrix} \right\}$$

$$B_1 = \text{diag}\left\{ \begin{bmatrix} b_1 \\ b_2 \\ 0 \\ 0 \end{bmatrix}, \begin{bmatrix} 0 & 0 \\ 0 & 0 \\ \tilde{b}_{31} & \tilde{b}_{32} \\ \tilde{b}_{41} & \tilde{b}_{42} \end{bmatrix} \right\}$$

$$B_2 = \text{diag}\left\{ \frac{V}{l} \begin{bmatrix} 1 \\ l_s \end{bmatrix}, \begin{bmatrix} 0 & 0 \\ 0 & 0 \\ \tilde{b}_{31} & \tilde{b}_{32} \\ \tilde{b}_{41} & \tilde{b}_{42} \end{bmatrix} \right\}$$

$$D_1 = \text{diag}\left\{ \begin{bmatrix} 0 \\ 0 \\ -V \\ 0 \end{bmatrix}, \begin{bmatrix} 0 \\ 0 \\ 0 \\ 0 \end{bmatrix} \right\}$$

$$D_2 = \text{diag}\left\{ \begin{bmatrix} -V \\ 0 \end{bmatrix}, \begin{bmatrix} 0 \\ 0 \\ 0 \\ 0 \end{bmatrix} \right\}$$

and

$$G_1(\Delta) = \text{diag}\left\{ \begin{bmatrix} g_1(\beta, r) \\ g_2(\beta, r) \\ 0 \\ 0 \end{bmatrix}, \begin{bmatrix} 0 \\ 0 \\ h_1(\beta, r) \\ h_2(\beta, r) \end{bmatrix} \right\}$$

$$G_2(\Delta) = \text{diag}\left\{ \frac{V}{l} \begin{bmatrix} 1 \\ l_s \end{bmatrix}, \begin{bmatrix} 0 \\ 0h_1(\beta, r) \\ h_2(\beta, r) \end{bmatrix} \right\}$$

where

$$h_1(\beta, r) = \tilde{h}_{31}\sigma_f c_f(\beta + \Delta_1(\beta, r)) + \tilde{h}_{32}\sigma_r c_r(\beta + \Delta_2(\beta, r)),$$

$$h_2(\beta, r) = \tilde{h}_{41}\sigma_f c_f(\beta + \Delta_1(\beta, r)) + \tilde{h}_{42}\sigma_r c_r(\beta + \Delta_2(\beta, r))$$

Now consider the problem of nonlinear state feedback  $H_\infty$  optimal control for Eq.(25), in which it is to find, if existing, the smallest value  $\gamma^* \geq 0$  such that for any  $\gamma > \gamma^*$  there exists a state feedback

$$u = l(x) \quad (26)$$

such that  $L_2$ - gain from  $d$  to  $[y^T, u^T]^T$  is less than or equal to  $\gamma$ , where the system (25) is said to have  $L_2$ - gain less than or equal to  $\gamma$  if

$$\int_0^T \|y\|^2 dt \leq \gamma^2 \int_0^T \|u\|^2 dt \quad (27)$$

for all  $T \geq 0$  and all  $u \in L_2(0, T)$ . For this problem formulation, we can apply the theorem proposed by A.J. van der Schaft[10, 11, 12]. Then, we obtain the following theorem.

**[Theorem 1]** Consider the nonlinear system with disturbances Eq.(25). Let  $\gamma > 0$ . Suppose there exists a  $C^\infty$  solution  $V \geq 0$  to the Hamilton-Jacobi equation

$$\begin{aligned} & \frac{\partial V(x)}{\partial x} Ax + \frac{1}{2} \frac{\partial V(x)}{\partial x} \left[ \frac{1}{\gamma^2} G(\Delta) G^T(\Delta) - B B^T \right] \\ & \times \left( \frac{\partial V(x)}{\partial x} \right)^T + \frac{1}{2} x^T C^T C x = 0, \quad V(x_0) = 0 \end{aligned} \quad (28)$$

or to the Hamilton-Jacobi inequality [13]

$$\begin{aligned} & \frac{\partial V(x)}{\partial x} Ax + \frac{1}{2} \frac{\partial V(x)}{\partial x} \left[ \frac{1}{\gamma^2} G(\Delta) G^T(\Delta) - B B^T \right] \\ & \times \left( \frac{\partial V(x)}{\partial x} \right)^T + \frac{1}{2} x^T C^T C x \leq 0, \quad V(x_0) = 0 \end{aligned} \quad (29)$$

then the closed-loop system for the feedback

$$u = -B^T \left( \frac{\partial V(x)}{\partial x} \right)^T \quad (30)$$

has  $L_2$ - gain (from  $d$  to  $[y^T, u^T]^T$ ) less than or equal to  $\gamma$ .

**(Proof)** Abbreviated.

The subscript  $i$  ( $= 1, 2$ ) in Eq.(25) is abbreviated in the Theorem 1.

#### 4.2 Suboptimal solution of Hamilton-Jacobi equation (inequality)

We consider the following linearized system derived from Eq.(25).

$$\begin{aligned}\dot{x}_i(t) &= A_i x_i(t) + B_i u(t) \\ &\quad + D_i \rho_{\text{ref}}(t) + E_i d_i(t) \\ y(t) &= C_i x_i(t), \quad (i = 1, 2)\end{aligned}\quad (31)$$

where  $E_i$ , ( $i = 1, 2$ ) is the first-order approximation of  $G_i(\Delta)$ , ( $i = 1, 2$ ). Then, we obtain the following corollary from Theorem 1.

**(Corollary 2)** Consider the linearized system (31) derived from the nonlinear steering system (25) and assume  $A_i$  is asymptotically stable. The  $L_2$  - gain of the linearized system (31) is less than or equal to  $\gamma$  if and only if there exists a solution  $P_i \geq 0$  of the algebraic Riccati equation

$$\begin{aligned}A_i^T P_i + P_i A_i + C_i^T C_i \\ + P_i \left( \frac{1}{\gamma^2} E_i E_i^T - B_i B_i^T \right) P_i = 0, \quad (i = 1, 2)\end{aligned}\quad (32)$$

The  $H_\infty$  optimal controller for Eq.(31), is given by [10, 11].

$$u(t) = -B_i^T P_i x_i(t), \quad (i = 1, 2). \quad (33)$$

**(Proof)** Abbreviated.

We suppose an approximate solution of the Hamilton-Jacobi equation (28), ((29)) as

$$V(x) = \frac{1}{2} x^T P x + V_h(x) \quad (34)$$

where  $P$  is a solution of the Riccati equation (32) and  $V_h(x)$  is satisfied the following higher order equation

$$\begin{aligned}-\frac{\partial V_h(x)}{\partial x} A_* x = \frac{1}{2} \frac{\partial V_h(x)}{\partial x} \left[ \frac{1}{\gamma^2} E E^T(\Delta) - B B^T \right] \\ \times \left( \frac{\partial V_h(x)}{\partial x} \right)^T + \frac{1}{2} \frac{\partial V(x)}{\partial x} G_h(x) \left( \frac{\partial V(x)}{\partial x} \right)^T\end{aligned}\quad (35)$$

where  $A_* := A - B B^T P + \frac{1}{\gamma^2} E E^T P$  and  $G_h(x)$  is the higher term of  $\frac{1}{\gamma^2} G(\Delta) G^T(\Delta) - B B^T$  in Eq.(28), (Eq.(29)). The  $m$ -th order terms  $V^{(m)}(x)$  of  $V(x)$ ,  $m = 3, 4, \dots$ , can be computed inductively starting from  $V^{(2)}(x) = \frac{1}{2} x^T P x$  by using the approximation scheme[12].

## 5 Numerical Simulations

In this section, we consider the numerical examples for the linearized system (31). The specification data of a typical passenger car is given in Table 1.

(1) The case 1:  $V = 15[m/sec]$ ,  $|\dot{V}| < 1$

The extended state space model for steering is obtained as follows.

$$\begin{aligned}\begin{bmatrix} \dot{\beta} \\ \dot{r} \\ \Delta \dot{\psi} \\ \dot{y}_s \end{bmatrix} &= \begin{bmatrix} -1.99 & -0.96 & 0 & 0 \\ 6.69 & 2.53 & 0 & 0 \\ 0 & 1 & 0 & 0 \\ 15 & 1.83 & 15 & 0 \end{bmatrix} \begin{bmatrix} \beta \\ r \\ \Delta \psi \\ y_s \end{bmatrix} \\ &+ \begin{bmatrix} 0.997 \\ 10.8 \\ 0 \\ 0 \end{bmatrix} \delta + \begin{bmatrix} 0 \\ 0 \\ -15 \\ 0 \end{bmatrix} \rho_{\text{ref}} \\ &+ \begin{bmatrix} g_1(\beta, r) \\ g_2(\beta, r) \\ 0 \\ 0 \end{bmatrix} \mu\end{aligned}\quad (36)$$

according to Eq.(21). The steering system (36) is unstable under no control. The bode diagram and impulse response of the steering system without any controller are shown by Figs. 7 and 8, respectively.

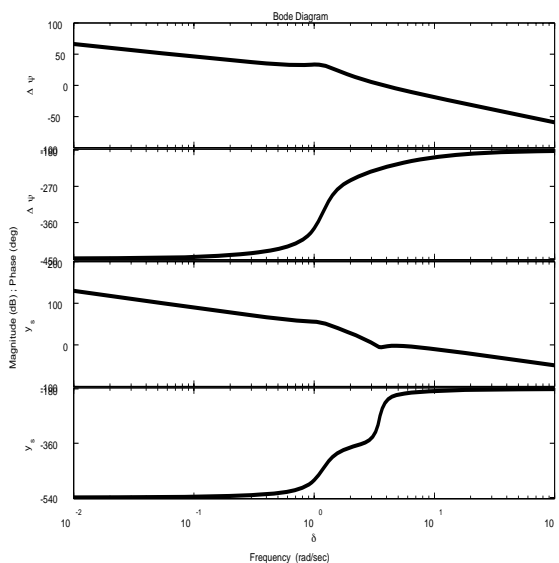


Fig. 7 Bode diagram of steering system without control (Case 1)

The  $H_\infty$  optimal control input for Eq.(36) with Eq.(22) is given by

$$\delta(t) = -[4.35 \ 1.29 \ 7.64 \ 1.0] \begin{bmatrix} \beta(t) \\ r(t) \\ \Delta \psi(t) \\ y_s(t) \end{bmatrix} \quad (37)$$



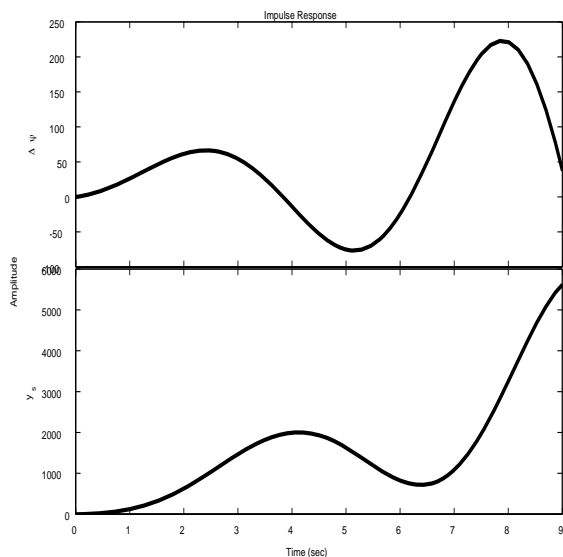


Fig. 8 Impulse response of steering system without control (Case 1)

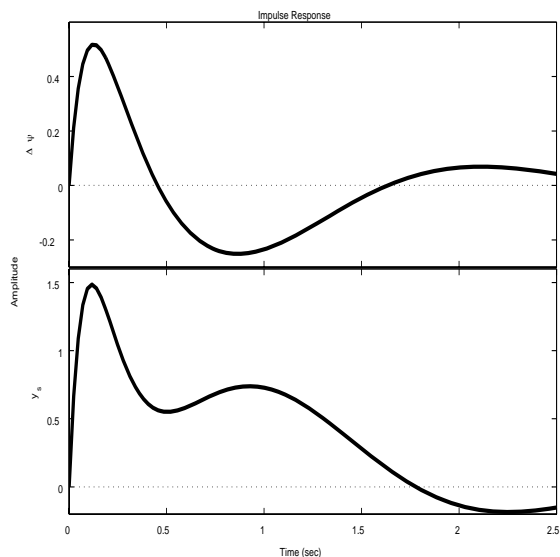


Fig. 10 Impulse response of steering system with the proposed controller (Case 1)

The bode diagram and impulse response of the steering system with the controller (37) are shown by Figs. 9 and 10, respectively.

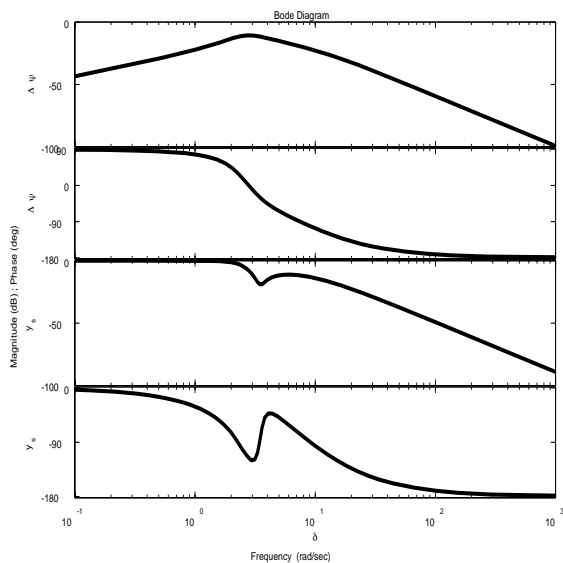


Fig. 9 Bode diagram of steering system with the proposed controller (Case 1)

For the vehicle automatic steering model (36) with the measurement system (22) and the controller (37). The proposed controller is tested in a simulation where the measurement output data are assumed to be obtained from a gyro (w.r.t. the yaw rate  $r$ ) and a GPS (w.r.t. the deviation  $y_s$  derived from the curvature  $\rho_{\text{ref}}$  of the prescribed reference path) each 2 seconds and the controller decides the steering angle  $\delta$  so that the deviation

$y_s$  is driven to zero and the yaw rate  $r$  follows  $V\rho_{\text{ref}}$ . The simulation result is shown in Fig. 11, which shows a good response on automatic steering control. Figure 11 shows responses of the linearized steering system (36) using an  $H_\infty$  optimal controller (37), where the output  $[\Delta\psi^T, y_s^T]^T$  is driven to zero as  $t \rightarrow \infty$  using the steering input  $\delta$  and the reference trajectory  $\rho_{\text{ref}}$ , under the recurrent disturbance.

Tab. 1 Data for a passenger car

$l$	=	2.54	[m]
$l_f$	=	0.97	[m]
$l_r$	=	1.57	[m]
$l_s$	=	1.83	[m]
$c_f$	=	25,000	[N/rad]
$c_r$	=	25,000	[N/rad]
$K_f$	=	20,000	[N/m]
$K_r$	=	18,000	[N/m]
$C_f$	=	1,500	[N·sec/m]
$C_r$	=	2,000	[N·sec/m]
$V$	=	15, ( or 0.05 )	[m/sec]
$m$	=	1,170	[kg]
$\mu$	=	0.7	
$i^2$	=	1.341	[m <sup>2</sup> ]

The state space model for the suspension system of a vehicle is obtained as follows.

$$\begin{bmatrix} \dot{z} \\ \dot{\theta} \\ \dot{w} \\ \dot{q} \end{bmatrix} = \begin{bmatrix} 0 & 0 & 1 & 0 \\ 0 & 0 & 0 & 1 \\ -32.48 & -7.57 & -2.99 & -1.44 \\ -5.65 & -40.27 & -1.07 & -4.04 \end{bmatrix}$$

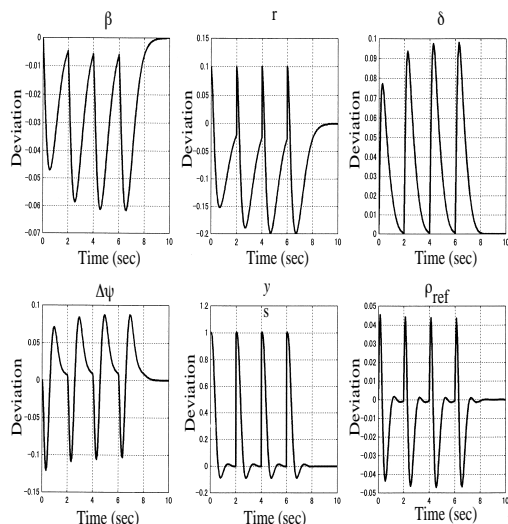


Fig. 11 State response and control sequence with automatic steering control (Case 1)

$$\begin{aligned}
 & \times \begin{bmatrix} z \\ \theta \\ w \\ q \end{bmatrix} \\
 & + \begin{bmatrix} 0 & 0 \\ 0 & 0 \\ 0.000855 & 0.000855 \\ -0.000618 & 0.001 \end{bmatrix} \begin{bmatrix} U_f \\ U_r \end{bmatrix} \\
 & + \begin{bmatrix} 0 \\ 0 \\ h_1(\beta, r) \\ h_2(\beta, r) \end{bmatrix} \mu \quad (38)
 \end{aligned}$$

according to Eq.(15). The suspension system (38) is stable. The  $H_\infty$  optimal control input for Eq.(38) with Eq.(17) is given by

$$\begin{aligned}
 \begin{bmatrix} U_f(t) \\ U_r(t) \end{bmatrix} &= \begin{bmatrix} -0.003 & 0.030 & -0.206 & 0.148 \\ -0.025 & 0.003 & -0.102 & -0.096 \end{bmatrix} \\
 & \times \begin{bmatrix} z(t) \\ \theta(t) \\ w(t) \\ q(t) \end{bmatrix} \quad (39)
 \end{aligned}$$

The bode diagram and impulse response of the suspension system with the controller (39) are shown by Figs. 12 and 13, respectively.

The numerical simulations with several kinds of active suspension systems are shown in Fig. 14[5].

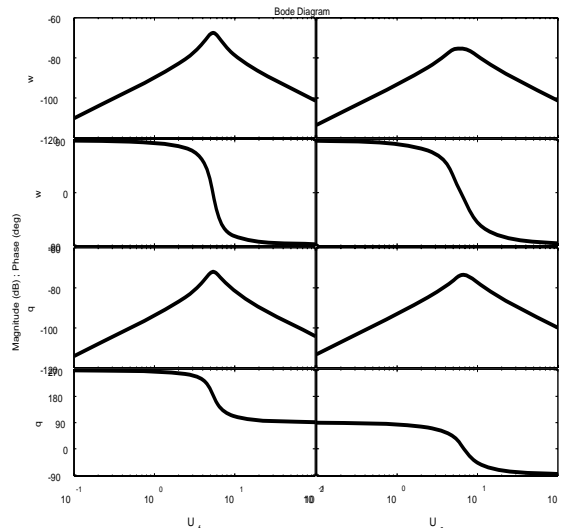


Fig. 12 Bode diagram of suspension system with the proposed controller (Case 1)

## 6 Conclusions

It has been considered the problem of automatic driving control of autonomous vehicles which includes the automatic steering control and the induced active suspension control. The extended model including small nonlinear factors of the steering motion, the induced bouncing motion and the induced pitching motion is derived. The  $H_\infty$  optimal controller for the extended driving system is introduced so that the autonomous vehicle can be driven along the reference path with riding stability.

The proposed controller is supposed to be considered for autonomous vehicles in which no passengers ride. For the autonomous vehicles with passengers, the proposed controller does not seem to give them a comfortable ride because there are many problems (oscillation and yawing, etc.) to be remained unsolved for a comfortable ride. Recently, the integrated control of each chassis control system such as active 4WS system, active 4WD system, anti-lock brake system and traction control system[1, 14, 15] is confirmed to have passed higher potential of vehicle dynamic performance and these control systems are applicable to the control of autonomous vehicles.

## 7 References

- [1] Y. Matsuo, H. Harada, M. Yamamoto, and Y. Kubota. Development of experimental vehicle with integrated chassis control. *Toyota Engineering*, 40:120–126, 1990.
- [2] K. Moriwaki. A method of automatic motion control with optimization. In et. al. H. Asama, editor, *Proceedings of the Fourth IFAC Symposium on Intelligent Autonomous Vehicles*, pages 393–

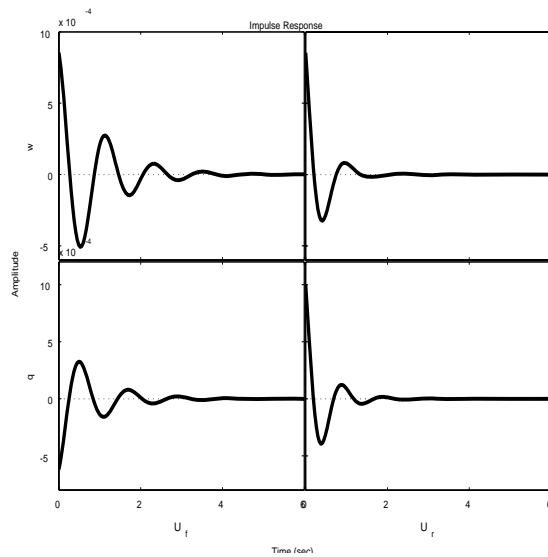


Fig. 13 Impulse response of suspension system with the proposed controller (Case 1)

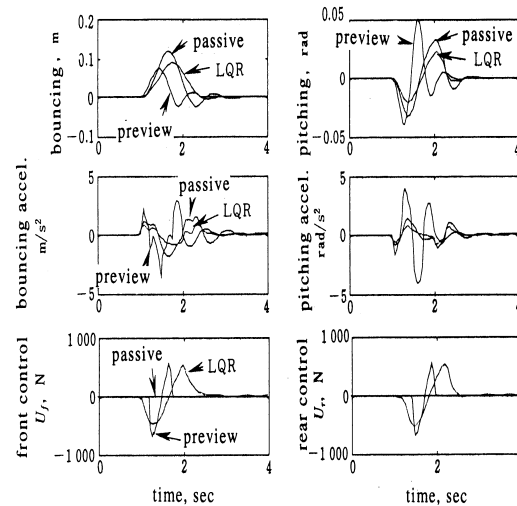


Fig. 14 State response and control sequence with active suspension control[5]

- 398, Sapporo, Hokkaido, Japan, September 2001. IFAC, Elsevier.
- [3] J. Ackermann, A. Bartlett, D. Kaesbauer, W. Sienel, and R. Steinhauser. *Robust Control Systems with Uncertain Physical Parameters*. Springer-Verlag, London, 1993.
- [4] M. Abe. *Vehicle Dynamics and Control*. Saikai-do Press, Tokyo, 1992.
- [5] M. Nagai, A. Okada, K. Komoridani, Y. Suda, K. Tani, H. Amijima, S. Nakajiro, H. Harada, M. Miyamoto, and H. Yoshioka. *Dynamics and Control of Vehicles*. Yoken-do Press, Tokyo, 1999.
- [6] R. Andrzejewski and J. Awrejcewicz. *Nonlinear Dynamics of a Wheeled Vehicle*. Springer, New York, 2005.
- [7] K. Kanai, Y. Ochi, and T. Kawabe. *Vehicle Control -Airplanes and Automotives-*. Maki Shoten, Tokyo, 2004.
- [8] J.R. Ellis. *Vehicle Dynamics*. Business Book Ltd., London, 1969.
- [9] K. Moriwaki and K. Tanaka. Motion control with optimization for autonomous vehicles. In *Proceedings of 2004 Japan - USA Symposium on Flexible Automation*, pages No.JS-27, Denver, Colorado, USA, June 2004.
- [10] K. Moriwaki. Autonomous steering control for electric vehicles using nonlinear state feedback  $h_\infty$  control. *Nonlinear Analysis*, 63:e2257-e2268, 2005.
- [11] A.J. van der Schaft.  $l_2$ -gain analysis of nonlinear systems and nonlinear state feedback  $h_\infty$  control. *IEEE Trans. on Automatic Control*, AC-37:770-784, 1992.
- [12] A.J. van der Schaft.  *$L_2$ -gain and Passivity Techniques in Nonlinear Control*. Springer-Verlag, London, 1996.
- [13] S. Boyd, L.E. Ghaoui, E. Feron, and V. Balakrishnan. *Linear Matrix Inequality in System and Control Theory*. SIAM, Philadelphia, 1994.
- [14] H. Minegishi, K. Ise, S. Tanaka, S. Katayama, Y. Inoue, and H. Miyazaki. Traction control system. *Journal of the Society of Automotive Engineers of Japan*, 42:1037-1044, 1988.
- [15] K. Nasukawa, Y. Miyashita, and M. Shiokawa. *Efficiency Tests for Running of Automotive Vehicles*. Sankai-do Press, Tokyo, 1993.